Phase Noise Spectral Density Measurement of Broadband Frequency-Modulated Radar Signals

Peter Tschapek, Georg Körner, Andreas Hofmann, Christian Carlowitz, *Member, IEEE*, and Martin Vossiek, *Fellow, IEEE*

***Abstract*— In continuous-wave (CW) radar systems, such as frequency-modulated (FMCW), frequency-stepped (FSCW), or orthogonal frequency-division multiplexing (OFDM) radar systems, the range and velocity uncertainty are significantly impaired by phase noise decorrelation. Therefore, radar designers require accurate knowledge of their synthesizers' phase noise profiles to assess and predict radar performance. However, commercial phase noise analyzers cannot determine phase noise during modulation, and this may differ notably from phase noise in the pure CW mode. Recent methods for FMCW phase noise analysis usually require comprehensive *a priori* knowledge of modulation parameter and are prone to systematic deviations. To overcome these issues, we propose a new approach based on differential analysis of subsequent time-domain measurements. This method retains, statistical phase noise information while reducing systematic influences. For the first time, less *a priori* signal knowledge is required, and the method works for nearly any kind of broadband signal modulation. The concept requires only a digitizer (e.g., an oscilloscope) and some digital signal processing. The proposed method is first experimentally tested with different phase-locked-loop (PLL)-based synthesizer phase noise profiles. The obtained phase noise profiles agree perfectly with the results of an established measurement system. After this proof of basic functionality, the unique phase noise analysis capability for BB modulated signals is demonstrated with PLL-generated FMCW signals. The results reveal a significant phase noise difference between the different setups and clearly show the capability and benefit of the novel phase noise spectral density measurement concept.**

***Index Terms*— Continuous-wave (CW) radar, frequency-modulated continuous-wave (FMCW) radar, phase locked loops, phase noise measurement, phase noise profiles.**

I. Introduction

In THE field of commercial radar technology (e.g., automotive, industrial, or aerospace) broadband continuous-wave (CW) radar systems, such as frequency-modulated (FMCW), frequency-stepped (FSCW), or orthogonal frequency-division multiplexing (OFDM) radar systems, are well established and are the preferred radar concept. In various forms and antenna configurations, these systems can measure the range and velocity [1]–[3] of targets with distances of up to several hundred meters. The performance of frequency-modulated CW radar systems is influenced by systematic nonlinearities [4] and phase noise [5]–[7]. In coherent radar systems, the influence of phase noise can usually be neglected, due to the range correlation effect [7], [8]. However, as the target range increases, decorrelation occurs, and the achievable accuracy of the target range and radial velocity estimation becomes increasingly poor. Particularly in the case of long-range measurements, phase noise leads to a reduction in the target signal power spectral density (PSD) and a notably reduced signal-to-noise ratio (SNR) in the beat spectra. The influences of phase noise were intensively investigated in [9] and [10]. Therefore, measuring of phase noise is very important for assessing and predicting the overall system performance. Various methods are available for measuring phase noise of microwave oscillators. For example, commercial products, such as spectrum analyzers or signal source analyzers, offer sophisticated phase noise measurements of narrowband/sinusoidal CW signals. These devices usually differ in their method of measuring phase noise. Some, such as spectrum analyzers, use direct methods, whereas signal source analyzers use techniques with phase detectors or two-channel cross correlation. These methods differ in terms of their sensitivity and dynamics, but they are all limited to measuring the phase noise of mono-frequency sinusoidal signals.

In contrast, phase-locked-loop (PLL)-based frequency synthesizers are used in many areas due to their flexible operation modes. In the past, the simplest way to measure the change in phase noise when operating a PLL in the FMCW mode was to measure it in the feedback path of the PLL in front of the phase detector. This was done by exploiting the fact that the feedback signal at the phase detector is available as a mono-frequency sinusoidal signal that can be measured directly with a commercial phase noise measurement device. In [11] and [12], the phase noise of the feedback signal during an FMCW chirp increases significantly compared to the mono-frequency CW operation mode. However, the measured phase noise spectra of the feedback signals at the phase detector do not correspond to the phase noise at the voltage-controlled oscillator (VCO) output. This is especially true during a sweep for the divider's transfer function, which inevitably changes continuously.

Manuscript received September 1, 2021; revised December 14, 2021; accepted January 22, 2022. Date of publication February 25, 2022; date of current version April 4, 2022. This work was supported by the German Research Foundation (DFG) within the project "New methodologies for analytically modeling and compensation of phase noise based distortions in continuous wave radar" under Grant VO 1453/33-1. *(Corresponding author: Peter Tschapek.)*

The authors are with the Institute of Microwaves and Photonics (LHFT), Friedrich-Alexander-Universität Erlangen-Nürnberg (FAU), 91058 Erlangen, Germany (e-mail: peter.tschapek@fau.de; georg.gk.koerner@fau.de; andreas.hofmann@fau.de; christian.carlowitz@fau.de; martin.vossiek@fau.de).

Color versions of one or more figures in this article are available at https://doi.org/10.1109/TMTT.2022.3148311.

Digital Object Identifier 10.1109/TMTT.2022.3148311

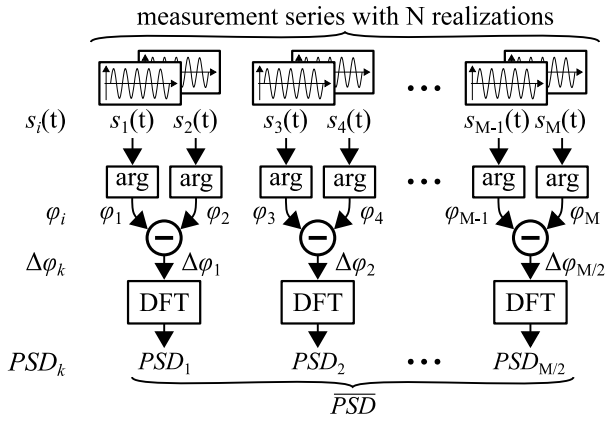

Fig. 1. Simplified illustration of the proposed approach. The measurement series consists of M realizations, of which two successive ones are calculated against each other. As a result, each calculation leads to a phase noise PSD. The average PSD over all spectra is finally calculated.

These methods also require direct access to the feedback path to measure the mono-frequency sinusoidal signal in front of the phase detector. However, the increasing integration depth of radar modules does not always allow for this possibility. In view of future developments in the field of software-defined radio (SDR) or phase-shifted keying (PSK), where only digital-to-analog converters (DACs) are used, a feedback path is no longer available.

A method for measuring the phase noise of FSCW chirps was first presented in [13], where a highly stable reference oscillator was used to down-convert the signals to the baseband (BB). Approaches are now available that can directly measure the phase noise PSD of FMCW chirps [14]. Both methods depend on *a priori* knowledge regarding their modulation parameters. For the FSCW case, the steps need to be at a precisely preselected position in time and height. For the FMCW case, the chirp needs to perform exactly as set up. Noise and systematic errors cannot be separated afterward.

In this article, we present a novel approach, illustrated in Fig. 1, that enables measurement of the phase noise of broadband frequency-modulated signals, in particular, FMCW signals, by differential demodulating a signal for direct measurement using a second measured signal. As each measurement contains all the information necessary for demodulation, except for the modulation duration, no further signal parameter estimation for demodulation is necessary in the proposed approach. The proposed approach is validated using a measurement series and different phase noise profiles, and it provides a reliable measurement of the phase noise of FMCW signals. To the best of our knowledge, no comparable measurement technique for measuring phase noise of broadband signals has been realized and validated in a similar manner in the literature.

The remainder of the article is organized as follows: Section II describes the theory and the new approach in detail. Section III discusses the validation. The description of the measurement setup and the measurement scenarios, as well as a discussion of the results, are given. Section IV demonstrates the new approach using a real PLL in the FMCW operation mode, followed by the conclusion.

II. Phase Noise Measurement of FMCW Chirps

In this section, the phase noise to be measured for frequency-modulated signals is defined, and the problems existing with classical approaches are specifically highlighted. Based on this, the new method and the solution to the problems addressed are presented.

A. Theory and Classical Approach

We first consider phase noise as a time-dependent phase term $\phi_{\text{Noise}}(t)$, which can be described by a stochastic and non-deterministic process. The phase of a mono-frequency sinusoidal CW signal $\phi_{\text{CW}}(t)$ superimposed by phase noise is then given by

$$\phi_{\text{Noisy}}(t) = \phi_{\text{CW}}(t) + \phi_{\text{Noise}}(t). \tag{1}$$

A real-value noisy mono-frequency sinusoidal signal is then described by

$$s_{\text{Noisy}}(t) = \sin(\omega_{\text{CW}} t + \phi_{\text{Noise}}(t)) \tag{2}$$

using (1), where the phase of the unaltered signal can be represented by

$$\phi_{\text{CW}}(t) = \omega_{\text{CW}} t = 2\pi f_{\text{CW}} t \tag{3}$$

where f_{CW} and ω_{CW} are the radio frequency (RF) and the angular frequency, respectively. However, as is well-known, the phase of a real-value signal cannot be determined exactly by the inverse trigonometric function arcsine. Therefore, the discrete Hilbert transform (DHT) is applied, and this makes possible the transformation of the real-value signal from (2) into the complex-value signal

$$s_{\text{Noisy}}(t) = \mathrm{e}^{\mathrm{j}(\omega_{\text{CW}} t + \phi_{\text{Noise}}(t))}. \tag{4}$$

The phase term $\phi_{\text{Noise}}(t)$ of interest for phase noise measurement can now be extracted with a simple demodulation using complex conjugate multiplication with an ideal signal

$$\begin{aligned} s_{\text{Noise}}(t) &= s_{\text{Noisy}}(t) \cdot s^*_{\text{Ideal}}(t) \\ &= \mathrm{e}^{\mathrm{j}(\omega_{\text{CW}} t + \phi_{\text{Noise}}(t))} \cdot \mathrm{e}^{-\mathrm{j}(\omega_{\text{Ideal}} t)}. \end{aligned} \tag{5}$$

Demodulation can also be performed directly by determining the difference between the two signals' arguments

$$\arg(s_{\text{Noise}}(t)) = (\omega_{\text{CW}} - \omega_{\text{Ideal}})t + \phi_{\text{Noise}}(t). \tag{6}$$

In reality, however, the carrier cannot be assumed to disappear completely in the course of demodulation. If the angular frequency estimated ω_{Ideal} for demodulation is not exactly equal to the angular frequency ω_{CW} of the mono-frequency sinusoidal signal component to be demodulated, that is

$$\Delta\omega = \omega_{\text{CW}} - \omega_{\text{Ideal}} \tag{7}$$

then the angular frequency difference $\Delta\omega$ remains in the phase results and (6) must be extended accordingly to

$$\arg(s_{\text{Noise}}(t)) = \Delta\omega t + \phi_{\text{Noise}}(t). \tag{8}$$

The angular frequency difference $\Delta\omega$ then leads to a linear phase variation over time. If the residual phase due to the

frequency deviation is significantly smaller than $\sigma(\phi_{\text{Noise}}(t))$, that is

$$\Delta\omega t \ll \sigma(\phi_{\text{Noise}}(t)) \tag{9}$$

then the approximation

$$\arg(s_{\text{Noise}}(t)) \approx \phi_{\text{Noise}}(t) \tag{10}$$

can be applied but this is not the expected case, where

$$\sigma(\phi_{\text{Noise}}(t)) = \sqrt{\frac{1}{T}\int_0^T \phi_{\text{Noise}}^2(t)\ \mathrm{d}t} \tag{11}$$

is the estimated standard deviation of the continuous zero-mean random variable $\phi_{\text{Noise}}(t)$. The theory can easily be extended to FMCW signals. The phase of an FMCW signal is

$$\phi_{\text{FMCW}}(t) = \phi_0 + \left(\omega_0 + \frac{1}{2}\mu t\right)t \tag{12}$$

with the initial phase ϕ_0, the start angular frequency ω_0 of the chirp, and the sweep rate μ, where the sweep rate is defined by

$$\mu = \frac{2\pi B}{T} \tag{13}$$

with the bandwidth B and the sweep time T. The demodulated phase, analogous to (6), is given by

$$\arg(s_{\text{Noise}}(t)) = \left(\omega_0 - \omega_{0,\text{Ideal}}\right)t + (\mu - \mu_{\text{Ideal}})t^2 + \phi_0 + \phi_{\text{Noise}}(t) \tag{14}$$

with the estimated parameters of the start angular frequency ω_0 and the sweep rate μ. For the ideal phase, which is a quadratic term in the FMCW signal compared to a linear term for a mono-frequency sinusoidal signal, two parameters, $\omega_{0,\text{Ideal}}$, the ideal start angular frequency, and μ_{Ideal}, the ideal sweep rate must now be estimated. As the sweep parameters cannot be determined exactly, a difference term of the form

$$\Delta\phi_{\text{FMCW}}(t) = \Delta\omega_0 t + \Delta\mu t^2 + \Delta\phi_0 \tag{15}$$

remains, where $\Delta\omega_0$ is the difference in the start angular frequency, and $\Delta\mu$ is the difference in the sweep rate. By non-idealities, in particular, systematic deviations, within a chirp, the phase (12) expands to

$$\phi_{\text{FMCW}}(t) = \phi_0 + \left(\omega_0 + \frac{1}{2}\mu t\right)t + \sum x_n \cdot t^n. \tag{16}$$

The occurring non-idealities are described with the sum of polynomials of the nth degree. The demodulated signal can be summarized as follows:

$$\arg(s_{\text{Noise}}(t)) = \Delta\omega_0 t + \frac{1}{2}\Delta\mu t^2 + \sum x_n \cdot t^n + \phi_{\text{Noise}}(t). \tag{17}$$

A classical parameter estimation approach would clearly boost the computational and experimental complexity substantially to guarantee accurate results.

State-of-the-art measurement methods, particularly the methods used in commercial products, are limited to mono-frequency sinusoidal signals and cannot handle modulated RF signals. Therefore, phase noise measurement of modulated RF signals is still the subject of research, as this requires correct demodulation.

In [13] and [14], highly stable reference oscillators were used to mix the chirp into the BB. The chirps measured in the BB can then be converted into an analytical signal using the DHT or applying In-phase and quadrature (IQ) demodulation, and the phase can be demodulated using an ideal phase. As a result, the remaining phase is defined as phase noise.

In [14], the phase noise PSD in the discrete domain was calculated with discrete Fourier transform (DFT) and subsequent scaling

$$\text{PSD} = \frac{1}{f_S N}|\text{DFT}\{\Delta\varphi(m)\}|^2 \tag{18}$$

where $\Delta\varphi(m)$ is the de-chirped digitized phase difference from the ideal parabolic phase course, and m describes the samples, and is an integer.

However, in the measurement principles based on the classical approach, we need to address two major challenges: separating systematic influences from stochastic influences and demodulating the radar signals of arbitrary modulation (e.g., FMCW). The former cannot be easily achieved with current approaches, because demodulation is performed with an ideal signal, which means that systematic components remain part of the signal and can be only partially reduced with expensive post-processing. In addition, demodulation requires knowledge about the modulation parameters and their temporal sequence, or they have to be estimated directly before digital signal processing (DSP). Especially with FSCW, this can lead to sophisticated reconstruction processes. As a result, both approaches need to know system parameters, such as the start frequency, bandwidth, or step size. The two issues lead to a new approach that provides solutions to both challenges.

B. Proposed Approach

Referring to probability theory, in the case of a stochastic process, where the process is time-dependent, the resulting time function or signal $s(t)$ is called the realization of the stochastic process. Consequently, in a series of measurements of signals, an ensemble of realizations $s_i(t)$ is created. The proposed approach requires a huge number of realizations of the radar signal to be investigated, and they are subject to the same stochastic process. This stochastic process and thus, the process of the phase $\phi_{\text{Noise}}(t)$ are cyclostationary processes for a time period T, which corresponds to the sweep time. Thus, the statistical properties are invariant for a time shift over bT, where b is an integer. At this point, no statement can be made regarding whether the phase noise is stationary during a ramp.

The phase of each realization of the frequency-modulated signals must be uncorrelated with all other realizations, and under consideration of the Nyquist criterion, must be low-pass filtered as a sampled time signal. Due to multiple sources of phase noise, we can assume that the central limit theorem [15] is satisfied and the phase noise can be assumed to be normally distributed and zero-mean in the time-domain. A generalized

version of (17) can be introduced as

$$\arg\big(s_{i,\mathrm{Noise}}(t)\big) = \sum_{n=0}^{N} x_{i,n}t^n + \phi_{i,\mathrm{Noise}}(t) + \phi_{i,0}. \tag{19}$$

The variable i is the counting index, and $\phi_{i,0}$ is a random start phase of the evaluated realization. An additional requirement (and this also applies to the methods used in commercial measuring instruments and in classical approaches) is that the mixing process does not alter the noise properties, and thus, in particular, it does not contribute additional phase noise. As a rule, however, highly stable local oscillators (LOs) already fulfill this requirement, if their phase noise is significantly lower (e.g., at least 10 dB lower) than the phase noise of the radar signals over most of the PSD. In addition, the noise floor of the oscilloscope, and thus the maximum achievable dynamic range due to quantization noise and other analog-to-digital converter (ADC) noise sources, must be taken into account. However, this can be estimated and measured in advance using established methods [16].

Under these conditions, the modulation parameters and the systematic influences of a measured chirp can be assumed to remain almost identical from realization to realization, described by

$$x_{i,n} = x_{i-1,n}. \tag{20}$$

The core of the idea (which can provide a solution to both challenges) is that we apply differential demodulation, which eliminates all systematic and therefore time-invariant signal components. Specifically, the phases of the two measurements are subtracted from each other. The result is one realization of the desired phase noise, as follows:

$$\begin{aligned}&\arg\big(s_{i,\mathrm{Noise}}(t)\big) - \arg\big(s_{i-1,\mathrm{Noise}}(t)\big)\\ &= \sum_{n=0}^{N}\big(x_{i,n} - x_{i-1,n}\big)\cdot t^n + \phi_{i,\mathrm{Noise}}(t) - \phi_{i-1,\mathrm{Noise}}(t) + \Delta\phi_0\\ &= \phi_{i,\mathrm{Noise}}(t) - \phi_{i-1,\mathrm{Noise}}(t) + \Delta\phi_0\end{aligned} \tag{21}$$

where $\Delta\phi_0 = \phi_{i,0} - \phi_{i-1,0}$ is the remaining difference of the random start phases $\phi_{i,0}$ and $\phi_{i-1,0}$.

Again, note that our goal is not an exact determination of the phase noise of a single measurement or single realization, but a determination of the average of the PSD of the phase noise over a series of measurements. To do this, we need only a few of random representations of the phase noise of individual realizations whose statistical properties are identical to those of a single measurement.

In detail, the steps of the new approach, illustrated in Fig. 1, are as follows: After digitalization, the DHT is used to calculate the analytical signal from all realizations, to get the extracted and unwrapped phase. Alternatively, the DHT can be skipped and the phase extracted directly from the measured data, provided that complex-value BB signals are available in the case of quadrature down-conversion. In the following, phase demodulation is done by calculating the difference between the phase of the current realization and the phase of the previous realization to minimize the influence of low-frequency phase noise ($\ll$ 1 kHz), also known as frequency drift of the PLL:

$$\Delta\phi_k(t) = \frac{1}{\sqrt{2}}\big(\phi_{i-1,\mathrm{Noise}}(t) - \phi_{i,\mathrm{Noise}}(t) + \Delta\phi_0\big). \tag{22}$$

The difference between two uncorrelated normally distributed processes increases the standard deviation by a factor of $\sqrt{2}$, and therefore, it must be corrected accordingly. This approach can also be extended to the calculation of any two realizations.

The difference between the two phases $\Delta\phi_0$ with different start phases $\phi_{i,0}$ and $\phi_{i-1,0}$ leads to a constant phase offset. The remaining offset is removed by subtracting the time average $\Delta\bar{\phi}_k(t)$ of $\Delta\phi_k(t)$:

$$\phi_k(t) = \Delta\phi_k(t) - \Delta\bar{\phi}_k(t). \tag{23}$$

In the following, the relation of the time interval between two measurements T_M to the signal duration T_S is of particular interest. As soon as $T_\mathrm{M} \gg T_\mathrm{S}$, low-frequency phase noise becomes more important in differential demodulation. The phase difference of the two measurements may show, in the case of mono-frequency signals, a slightly linear phase drift, or in the case of frequency-modulated signals, a slightly quadratic phase drift as a consequence of the frequency drift of the oscillator. This oscillator drift is characterized by a very high peak at the first frequency bin in the phase noise PSD. However, the first frequency bin increase caused by this effect is not part of the phase noise to be investigated, which occurs during T_S, and must be eliminated. To reduce this problem, a first-degree polynomial fit p_1 is obtained from $\phi_k(t)$ and is applied to compensate a linear phase difference

$$\phi_k(t) = \phi_k(t) - p_1(\phi_k(t)). \tag{24}$$

This operation significantly reduces the influence of long-term phase noise (frequency drift).

Now we switch to the discrete time domain to define the PSD for a discrete phase, as will be the case when we evaluate the collected data. Thus, $\phi_k(t)$ becomes $\phi_k[m]$, where m describes the samples of the digitized remaining phase under investigation. The results of $\phi_k[m]$ are transformed into the frequency domain with the DFT normalized. It represents the phase noise PSD_k of two measurements and leads to

$$\mathrm{PSD}_k = \frac{1}{f_\mathrm{S}N}|\mathrm{DFT}\{\phi_k[m]\}|^2 \tag{25}$$

where f_S is the sampling frequency of the oscilloscope and N the number of samples of $\phi_k[m]$. When calculating the phase noise PSD, the extraction of the phase automatically implies the assumption of small-angle approximation and normalization to the carrier in one step. The PSD obtained in (25) is an inconsistent estimator of the spectral density. Accordingly, the variance in the PSD is independent of the length N of the DFT and thus scatters strongly around the expected value. However, for a single realization of a signal, the variance of the PSD can be reduced by segmentation at the expense of spectral resolution. The Blackman-Tukey, Bartlett, and Welch methods are relevant. However, if several realizations of a signal are available and are part of the same cyclostationary stochastic process, as in our scenarios, then the

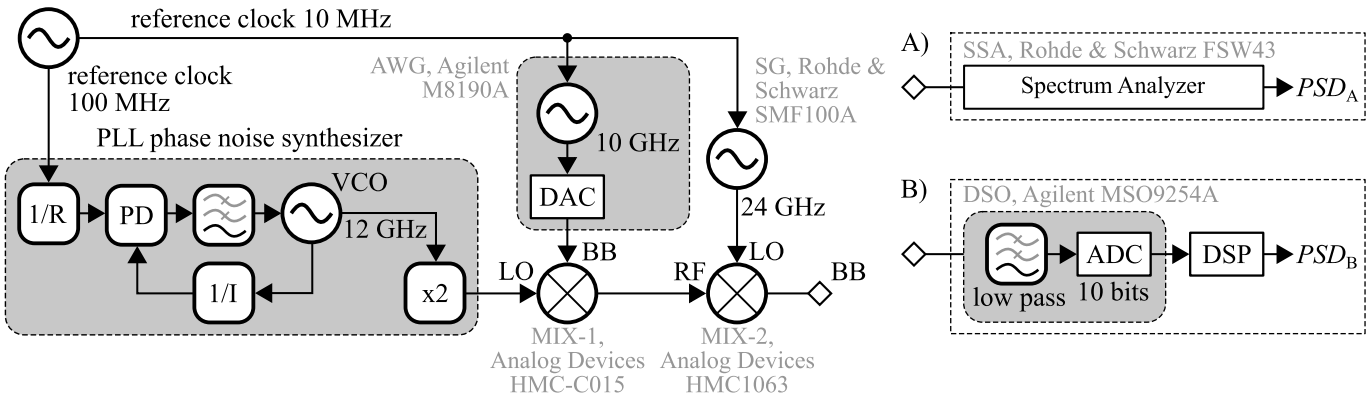

Fig. 2. Experimental verification setup for phase noise measurement. The phase noise of the signals at the output of the MIX-2 are measured either via measurement setup A) using a spectrum analyzer or via measurement setup B) using an oscilloscope and DSP. The connection line of the reference clock at the DSO and the SSA is not drawn in the figure. Furthermore, the trigger signal between the AWG and the DSO is not drawn.

variance in the PSD-describing process can be significantly reduced by averaging several PSDs, while maintaining the spectral resolution. In our implementation, the final phase noise PSD, which is the average of the normalized power of the phase noise in the frequency domain, is obtained by averaging all processed realizations

$$\overline{\mathrm{PSD}} = \frac{1}{K}\sum_{k=1}^{K}\left(\frac{1}{f_S N}|\mathrm{DFT}\{\phi_k[m]\}|^2\right). \tag{26}$$

Equation (26) is comparable to the measured PSD generated by commercial phase noise measurement devices.

At this point, we would like to discuss the various factors that significantly influence the achievable measurement accuracy of the proposed approach. First, the modulation period of the signal under investigation determines the time length of the realizations and thus the minimum bin spacing Δf_{DFT} in a discrete spectrum. The bin spacing, and therefore the resolution of near carrier information, is directly dependent on the temporal signal length T_S and is described by the relationship

$$\Delta f_{\mathrm{DFT}} = 1/T_S. \tag{27}$$

The variance in the PSD can be influenced only by the number of realizations and determines how accurately the expected value of the power density can be estimated. The measurement result depends on the delay between the chirps, because the delay may have an influence on random fluctuations. Therefore, the measurement configuration must be adapted to the radar scenario for which an accurate result is desired. The noise floor, which limits the measurement capability in particular far from the carrier, is significantly influenced by the quantization noise of the oscilloscope and thus by the vertical bit resolution of the ADC. The higher the vertical resolution, the lower the phase noise contributions; in particular, signals with very low phase noise can be measured. Furthermore, the noise property of the signal generator used for down-converting the radar signal to the BB limits the measurement accuracy and forms a lower sensitivity limit.

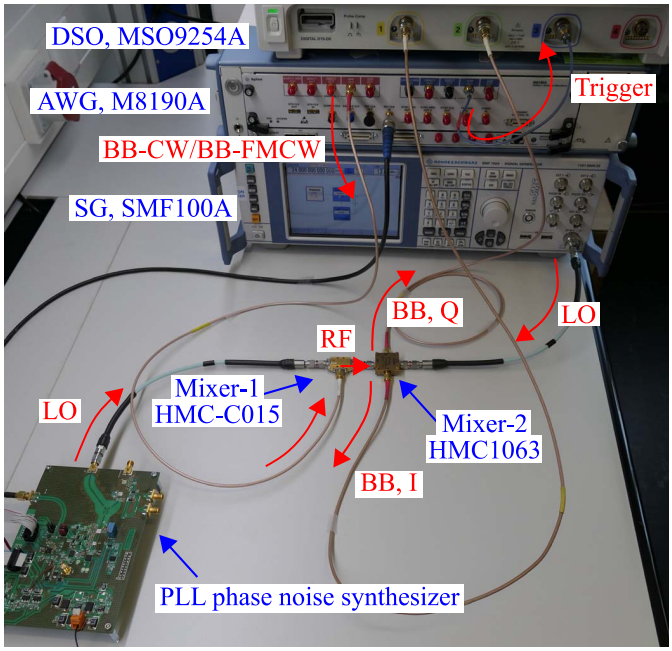

Fig. 3. Experimental verification implementation. Setup B) is shown.

III. Experimental Verification

As described in the previous section, in commercial measuring instruments, phase noise can be determined only from mono-frequency sinusoidal signals. For verification of the proposed method, a signal and spectrum analyzer (SSA, Rohde & Schwarz FSW43) with integrated phase noise measurement is used as a reference. Therefore, the concept used is presented, followed by verification of the proposed approach with mono-frequency sinusoidal signals (scenario 1), and finally, by verification using FMCW signals (scenario 2).

A. Concept and Setup for Experimental Verification

The proposed approach was tested using the measurement setup shown in Figs. 2 and 3. The measurement setup is based on the following concept to ensure verification: The phase noise to be measured must be independent of the modulation

TABLE I
PLL PRESCALER PARAMETER FOR EXPERIMENTAL VERIFICATION

Name	R	I	f_{PD}
R1	1	30	100 MHz
R4	4	120	25 MHz
R16	16	480	6,25 MHz

of the radar signal in the BB. For this purpose, a high-precision signal generator (SG, Rohde & Schwarz SMF100A) and an arbitrary waveform generator (AWG, Agilent M8190A) for a DAC enabling arbitrary modulations are used. Both devices have very low phase noise profiles and high-frequency stability. The SG has phase noise < -96 dBc/Hz@1 kHz at a carrier frequency of 24 GHz, while the AWG has phase noise <-103 dBc/Hz@1 kHz at a generated carrier frequency of 750 MHz. This means that they will not have a visible impact on phase noise measurement, because the phase noise of the PLL is at least 6 dB higher at 1 kHz, and the difference increases significantly with the increasing offset frequency up to 1 MHz. The digital sampling oscilloscope (DSO, Agilent MSO9254A) used in this setup is a DSO with a 2.5-GHz analog bandwidth.

A PLL transceiver board specially developed at our institute allow us to realize different phase noise profiles with different prescalers R and I, as listed in Table I. The PLL operates in integer mode. The two prescalers influence the transfer function of the PLL, allowing the phase noise to be adjusted as shown in Fig. 2. This allows the generation of different phase noise profiles; thus, their measurement with different setups allows comparison of the setups. The transceiver board represents the phase noise synthesizer to be measured, where the synthesizer parameters are assumed to be constant. The output frequency of the VCO is multiplied to 24 GHz by a frequency multiplier. The PLL gets its reference frequency from a high-precision 100-MHz reference clock.

The setup in Fig. 2 operates as follows: The PLL is in mono-frequency sinusoidal integer mode at 24 GHz and serves as a noisy LO on the first mixer (MIX-1, Analog Devices HMC-C015). The signal sources, the AWG and the SG, and the measurement devices, the SSA and the DSO are synchronized with a high-precision 10-MHz reference clock. At the MIX-1, the AWG can modulate any signal with low noise on the noisy carrier, meaning the phase noise should not change substantially when switching from a mono-frequency sinusoidal signal to an FMCW signal and can serve as a BB input signal. Thus, the two BB signals of the AWG used for verification are mono-frequency sinusoidal signals (BB-CW) and frequency-modulated signals (BB-FMCW). A second mixer (MIX-2, Analog Devices HMC1063) serves as a down-converter. For the mixing process, the SG outputs a mono-frequency sinusoidal signal at 24 GHz to convert the RF signals modulated by the AWG to the BB. The BB signals can be measured with a spectrum analyzer, which directly generates a phase noise spectrum of a mono-frequency sinusoidal signal, or with an oscilloscope in the time domain to enable our processing approach.

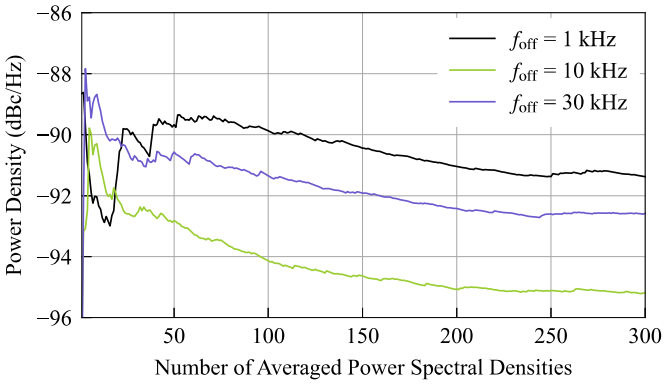

Fig. 4. Calculated mean value of scenario 1 B) BB-CW: R1 as a function of the number of PSDs used in the calculation. The results are shown exemplarily for 1-, 10-, and 30-kHz offset frequency up to 300 averaged densities.

With the DSO, the signal processing is as follows: The data are recorded with a sampling rate of 5 GSa/s without decimation at an analog bandwidth of 2.5 GHz. The measuring time is 1 ms in each case. The set effective vertical resolution is 10 bits for all measurements. The start of each measurement is defined by a trigger signal from the AWG. The recorded data are then transferred to a computer, where they are signal processed according to Fig. 1.

With this setup, two major scenarios with three different phase noise profiles (R1, R4, and R16) can be distinguished:

1) In the first scenario (scenario 1), the new approach is validated using mono-frequency sinusoidal signals and verified with a spectrum analyzer with integrated phase noise measurement. As the device tested does not change from A) to B), and the signal is dominated by the noise of the PLL, the PSD for a single setting has to be nearly the same;
2) The second scenario (scenario 2) is used to verify the proposed approach with FMCW signals created by the AWG. As the AWG has low phase noise, this modulation does not substantially change the phase noise at the output. Large differences in PSD indicate a measurement of unrelated signal parts.

The designation of the noise profiles is based on the integer value of the prescaler R of the reference input of the PLL. The phase comparison at the phase detector (PD), which is shown in Fig. 2 between the reference phase and the feedback phase, therefore takes place at 100 MHz for phase noise profile R1 with $R = 1$, at 25 MHz with $R = 4$ for R4, and at 6.25 MHz for R16 with $R = 16$. The different parameters are listed in Table I. Accordingly, integer prescaler I of the feedback path must be increased, and this also increases the phase noise. Therefore, different phase noise profiles can be realized without changing the output frequency. In both scenarios, 200 time signals (realizations), each with a signal duration of 1 ms, are acquired and evaluated for each of the three-phase noise profiles to generate the PSD. The averaging process of the PSD of the phase noise profile R1 is shown for three offset frequencies in Fig. 4. As can be seen from the curves in Fig. 4,

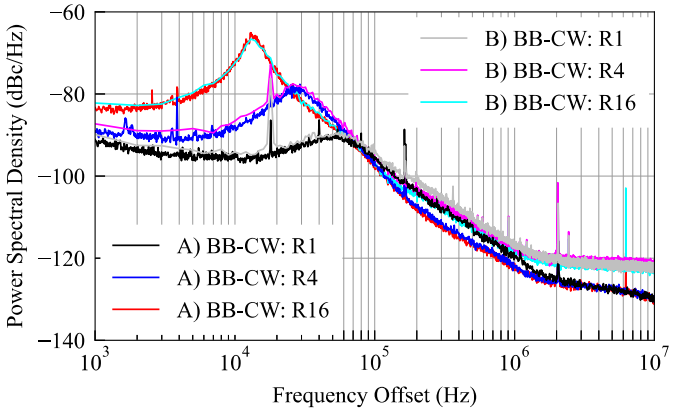

Fig. 5. Scenario 1: Comparison of the measured phase noise PSD for three different phase noise profiles (profiles R1, R4, and R16 are adjusted with different PLL prescaler values as illustrated in Table I) and with two different measurement setups, the spectrum analyzer in A) and the proposed setup in B).

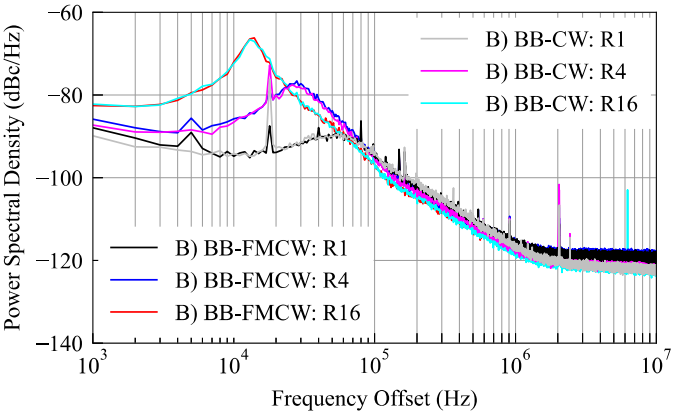

Fig. 6. Scenario 2: Comparison of the measured phase noise PSD with the proposed approach for three different phase noise profiles (profiles R1, R4, and R16 are adjusted with different PLL prescaler values, as illustrated in Table I) for two differently modulated BB signals (BB-CW and BB-FMCW).

the number of averaged densities should not be below 100 in order to obtain a meaningful PSD.

B. Scenario 1: Mono-Frequency Modulation

Fig. 5 shows the results of scenario 1 for the phase noise PSD of the measurement setup shown in Fig. 2. The mono-frequency sinusoidal signals generated by the AWG have a frequency of $f_{\mathrm{CW}} = 100$ MHz. The spectra are plotted as a function of the offset frequency. The spectra with the same profile clearly match very well, whether obtained with setup A) or with setup B). The proposed approach thus provides very good results, especially for noise components close to the carrier. Therefore, the methodology was verified in this respect for mono-frequency sinusoidal signals.

C. Scenario 2: FMCW Modulation

Fig. 6 shows the results of scenario 2 for the phase noise PSD of the measurement setup shown in Fig. 2. Again, the spectra, which represent the average of 200 realizations, are plotted as a function of the offset frequency. The FMCW chirps generated by the AWG have a bandwidth of 500 MHz and consist of up-chirps with corner frequencies $f_{\mathrm{Start}} = 100$ MHz and $f_{\mathrm{Stop}} = 600$ MHz. The mono-frequency sinusoidal signals created by the AWG are at $f_{\mathrm{CW}} = 100$ MHz.

The spectra of the same profile but different modulation clearly match very well. Accordingly, the modulation of the BB signal has no influence on the evaluation method. The proposed approach also allows the measurement of phase noise for modulated signals (e.g., FMCW). Thus, the method was also experimentally verified for modulated BB signals and confirmed the proposed approach. The peaks in Fig. 5, as well as in Fig. 6, are due to spurs of the PLL.

TABLE II
PLL PRESCALER PARAMETER FOR FMCW FRACTIONAL MODE

Name	R	I_{Start}	F_{Start}	I_{Stop}	F_{Stop}
R1	1	30	0.125	30	0.75
R4	4	120	0.5	123	0.0
R16	16	482	0.0	492	0.0

IV. Phase Noise Measurement of FMCW Chirp

Our aim with this measurement setup was to measure a real-world application of an FMCW radar chirp generated by the PLL at the output. For this purpose, the PLL was configured to different modes: mono-frequency sinusoidal integer mode (CW integer mode), mono-frequency sinusoidal fractional mode (CW fractional mode), and frequency-modulated fractional mode (FMCW fractional mode). The FMCW mode was examined in a different measurement setup, and its phase noise was measured with the proposed approached measurement method and compared to the CW integer and CW fractional modes.

A. Measurement Setup

The measurement setup is depicted in Fig. 7 and is similar to the previous measurement setup, with the exception of the AWG. Again, the components, the SG, the DSO, and the SSA are synchronized with each other via a high-precision 10-MHz reference clock. The PLL gets its reference frequency from a high-precision 100-MHz reference clock. If the PLL operates in the FMCW fractional mode, then the PLL directly generates automatic 1-ms upchirps from 24.1 to 24.6 GHz using a delta-sigma modulator. The integer and fractional divisors (I and F, respectively) used for this purpose are the start and stop parameters of the chirps and are listed in Table II. Two different phase noise profiles are divided again by choosing the prescaler path with $R = 1$, 4, and 16; see Table II. The MIX-2 and SG each serve as a mixer and a high-stability LO, respectively, for the down-conversion process. The LO feeds the mixer with a 24-GHz mono-frequency sinusoidal signal, thus performing a mixing process.

The upchirps present in the BB were then acquired with an oscilloscope, triggered by the PLL with 5 GSa/s and

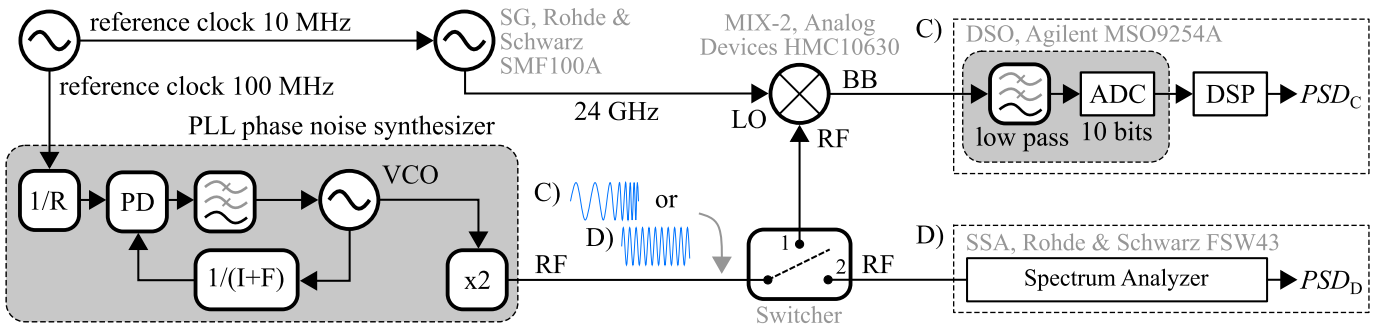

Fig. 7. Experimental setup for measuring the phase noise of a PLL in the CW integer, CW fractional, and FMCW fractional modes. If the PLL is operated in the FMCW mode, then switcher position 1 is selected for the duration of the measurement series, and the measurement data are evaluated via measurement setup C). Switcher position 2 is used for the PLL in the CW integer and CW fractional modes to directly feed the RF mono-frequency sinusoidal signals to the spectrum analyzer and is declared measurement setup D). The connection line of the reference clock at the DSO and the SSA is not drawn in the figure. Furthermore, the trigger signal between the PLL and the DSO is not drawn.

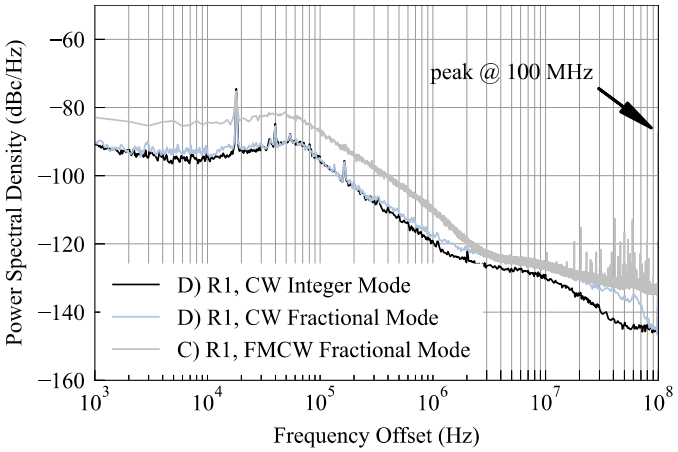

Fig. 8. Comparison of measured phase noise profile R1 from the PLL in the CW integer, CW fractional, and FMCW fractional modes. The spectra were determined using measurement setup D) in the CW integer and CW fractional modes and measurement setup C) in the FMCW fractional mode.

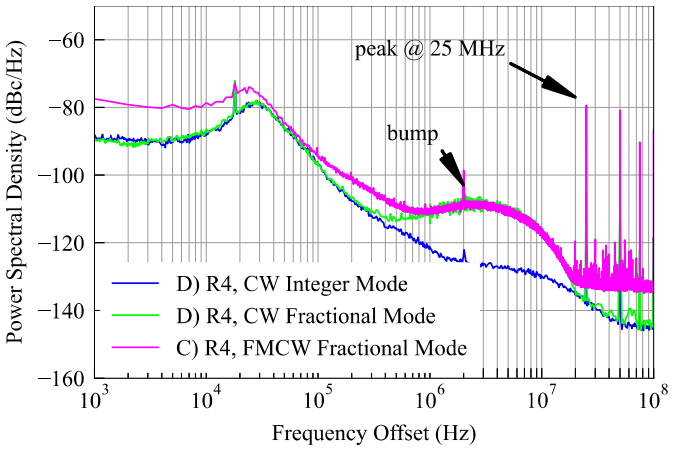

Fig. 9. Comparison of measured phase noise profile R4 from the PLL in the CW integer, CW fractional, and FMCW fractional modes. The spectra were determined using measurement setup D) in the CW integer and CW fractional modes and measurement setup C) in the FMCW fractional mode.

effective 10 bits as 1-ms-long time signals. For signal processing, 200 measurements per phase noise profile were again acquired and processed. The corresponding measurement setup is shown in Fig. 7 as measurement setup C). For comparison, the PLL was operated for 24-GHz mono-frequency sinusoidal signals in the CW integer and CW fractional modes. A delta-sigma modulator is always used in the fractional mode, in the CW fractional mode, and in the FMCW fractional mode. The PSD of the phase noise in both CW modes was measured using a spectrum analyzer. The corresponding measurement setup is shown in Fig. 7 as measurement setup D).

B. Results

Figs. 8–10 show the results of the PSD measurements of the phase noise of the PLL in different operating modes (CW integer, CW fractional, and FMCW fractional). Starting with the PLL phase noise results in the CW integer mode, this mode has the lowest phase noise for all three profiles (black, blue, and red curves). The phase noise curves for profiles R1, R4, and R16 in the CW fractional mode (gray-blue, green, and orange curves) agree well with those in the CW integer mode

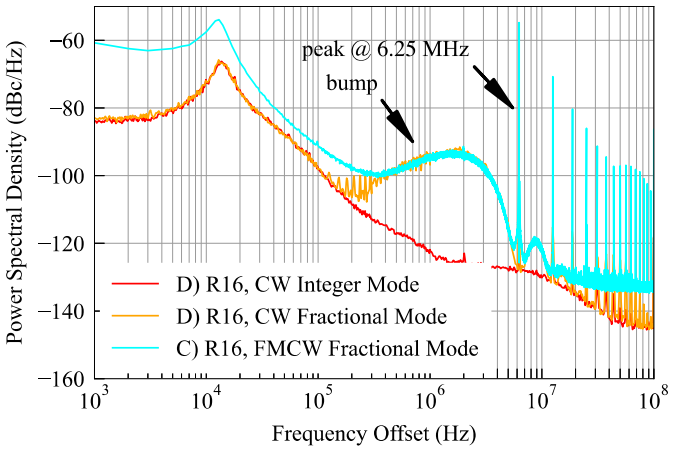

Fig. 10. Comparison of measured phase noise profile R16 from the PLL in the CW integer, CW fractional, and FMCW fractional modes. The spectra were determined using measurement setup D) in the CW integer and CW fractional modes and measurement setup C) in the FMCW fractional mode.

up to several hundred kilohertz. At higher offset frequencies, the curves differ, and especially for profiles R4 and R16, clear spurs can be seen whose offset frequencies correspond

to integer multiples of the reference frequency present and divided at the phase detector. In Fig. 9, which shows the results of profile R4, the first spur is at 25 MHz; in Fig. 10, the results of profile R16, the first spur appears at 6.25 MHz around the carrier. Characteristic bumps can be seen around the spurs in each case; these bumps were shown to some extent in [17] and were attributed to the use of the delta-sigma modulator.

The results of the phase noise of the PLL in the FMCW fractional mode show, particularly near the carrier, clearly higher phase noise for all three profiles in comparison to the CW integer and CW fractional modes (gray, magenta, and cyan). In some cases, the phase noise increases more than 12 dB. For the R4 and R16 profiles, pronounced spurs and bumps around the spurs are clearly visible.

The curves between the FMCW fractional and CW fractional modes match well in the area of the spurs and bumps; therefore, the course of the phase noise during a chirp can be attributed to the influence of the delta-sigma modulator. Accordingly, the rise close to the carrier must be assigned to the sweep process. At this point, it should be emphasized that the results represent phase noise at the output of an oscillator in frequency-modulated mode. The measurement method does not allow any conclusions which sources of phase noise are involved.

V. Conclusion

This article introduces a method that uses differential demodulation to measure phase noise of broadband frequency-modulated signals. The differential approach eliminates the need to estimate the modulation parameters or to have knowledge about them, with the exception of the modulation duration. Thus, the method is independent of the modulation. The method is most suitable for cases where the modulation parameters are invariant from realization to realization.

Nevertheless, one point that should be emphasized is that at least two realizations are needed for demodulation. The method is also limited to the bandwidth and memory size of current oscilloscopes, which means that only BB signals can be evaluated. In addition, the need for a low variance in the PSD requires several realizations. Thus, variant influences, such as frequency drift or mismatch between the modulation parameters of two realizations, become increasingly important. Therefore, these influences should be modeled in the context of a PLL simulation to enable an accurate estimation of the performance of this new measurement method. Frequency drift manifests in the PSD through excessively high peaks of the frequency bins close to the carrier. An additional processing step is required to eliminate this effect for long measurement series. For signal sources with low-frequency drift, demodulation between different realizations would be conceivable without frequency drift compensation. It should be noted that the measurement method must be adapted to the radar scenario. Especially for the time sequence of frequency-modulated radar signals, the measurement method must be adapted to this time sequence in order to reproduce delay-dependent effects.

Radar accuracy is critically affected by noise close to the carrier and the integrated area under the profiles [9], [10]. The deviations from common mono-frequency sinusoidal measurement methods shown in Figs. 8–10 may therefore be very important for future accuracy statements and should be investigated. The proposed approach provides an interesting alternative to classical approaches that rely on parameter estimation for demodulation.

References

[1] F. Roos, J. Bechter, C. Knill, B. Schweizer, and C. Waldschmidt, "Radar sensors for autonomous driving: Modulation schemes and interference mitigation," *IEEE Microw. Mag.*, vol. 20, no. 9, pp. 58–72, Sep. 2019, doi: 10.1109/MMM.2019.2922120.

[2] E. Miralles *et al.*, "Multifunctional and compact 3D FMCW MIMO radar system with rectangular array for medium-range applications," *IEEE Aerosp. Electron. Syst. Mag.*, vol. 33, no. 4, pp. 46–54, Apr. 2018, doi: 10.1109/MAES.2018.160277.

[3] L. Piotrowsky, T. Jaeschke, S. Kueppers, J. Siska, and N. Pohl, "Enabling high accuracy distance measurements with FMCW radar sensors," *IEEE Trans. Microw. Theory Techn.*, vol. 67, no. 12, pp. 5360–5371, Dec. 2019, doi: 10.1109/TMTT.2019.2930504.

[4] M. Pichler, A. Stelzer, P. Gulden, and M. Vossiek, "Influence of systematic frequency-sweep non-linearity on object distance estimation in FMCW/FSCW radar systems," in *Proc. 33rd Eur. Microw. Conf.*, Oct. 2003, pp. 1203–1206, doi: 10.1109/EUMA.2003.340795.

[5] F. Herzel, D. Kissinger, and H. J. Ng, "Analysis of ranging precision in an FMCW radar measurement using a phase-locked loop," *IEEE Trans. Circuits Syst., I, Reg. Papers*, vol. 65, no. 2, pp. 783–792, Feb. 2018, doi: 10.1109/TCSI.2017.2733041.

[6] M. El-Shennawy, B. Al-Qudsi, N. Joram, and F. Ellinger, "Fundamental limitations of phase noise on FMCW radar precision," in *Proc. IEEE Int. Conf. Electron., Circuits Syst. (ICECS)*, Dec. 2016, pp. 444–447, doi: 10.1109/ICECS.2016.7841234.

[7] F. Herzel, H. J. Ng, and D. Kissinger, "Modeling of range accuracy for a radar system driven by a noisy phase-locked loop," in *Proc. Eur. Radar Conf. (EURAD)*, Oct. 2017, pp. 521–524, doi: 10.23919/EURAD.2017.8249262.

[8] M. C. Budge and M. P. Burt, "Range correlation effects in radars," in *Proc. Rec. IEEE Nat. Radar Conf.*, Apr. 1993, pp. 212–216, doi: 10.1109/NRC.1993.270463.

[9] K. Thurn, R. Ebelt, and M. Vossiek, "Noise in homodyne FMCW radar systems and its effects on ranging precision," in *IEEE MTT-S Int. Microw. Symp. Dig.*, Jun. 2013, pp. 1–3, doi: 10.1109/MWSYM.2013.6697654.

[10] R. Ebelt, D. Shmakov, and M. Vossiek, "The effect of phase noise on ranging uncertainty in FMCW secondary radar-based local positioning systems," in *Proc. 9th Eur. Radar Conf.*, Oct. 2012, pp. 258–261.

[11] Y. Pan and J. Xu, "Phase noise analysis of fractional-N PLL based frequency ramp generator for FMCW radar," in *Proc. Asia–Pacific Microw. Conf. (APMC)*, Dec. 2015, pp. 1–3, doi: 10.1109/APMC.2015.7413554.

[12] A. Ergintav, F. Herzel, D. Kissinger, and H. J. Ng, "An investigation of phase noise of a fractional-N PLL in the course of FMCW chirp generation," in *Proc. IEEE Int. Symp. Circuits Syst. (ISCAS)*, 2018, pp. 1–4, doi: 10.1109/ISCAS.2018.8351072.

[13] A. Stelzer, K. Ettinger, J. Hoftberger, J. Fenk, and R. Weigel, "Fast and accurate ramp generation with a PLL-stabilized 24-GHz SiGe VCO for FMCW and FSCW applications," in *IEEE MTT-S Int. Microw. Symp. Dig.*, Jun. 2003, pp. 893–896, doi: 10.1109/MWSYM.2003.1212513.

[14] A. C. J. Samarasekera, R. Feger, J. Bechter, and A. Stelzer, "Phase noise measurements in chirped FMCW radar signals," in *IEEE MTT-S Int. Microw. Symp. Dig.*, Nov. 2020, pp. 1–4, doi: 10.1109/ICMIM48759.2020.9299035.

[15] T. M. Cover and J. A. Thomas, *Elements of Information Theory*, 2nd ed. Hoboken, NJ, USA: Wiley, 2006.

[16] C. Pearson, "High speed analog to digital converter basics," Texas Instrum. Corp., Dallas, TX, USA, Appl. Note SLAA510, 2011.

[17] A. Ergintav, F. Herzel, G. Fischer, and D. Kissinger, "A study of phase noise and frequency error of a fractional-N PLL in the course of FMCW chirp generation," *IEEE Trans. Circuits Syst. I, Reg. Papers*, vol. 66, no. 5, pp. 1670–1680, May 2019, doi: 10.1109/TCSI.2018.2880881.

Peter Tschapek received the B.Sc. degree in biomedical engineering from Technische Universität Ilmenau, Ilmenau, Germany, in 2014, and the M.Sc. degree in medical engineering from the Friedrich-Alexander-Universität Erlangen-Nürnberg (FAU), Erlangen, Germany, in 2016. He is currently pursuing the Ph.D. degree at the Institute of Microwaves and Photonics (LHFT), FAU.

In 2017, he joined BLAU Optoelektronik GmbH, Überlingen, Germany, where he worked as a Development Engineer in the field of testing and measurement of photonic devices. In 2018, he joined LHFT, FAU. His research interests include radar signal processing, especially synthesizer phase noise and microwave photonics.

Georg Körner received the B.Eng. degree in electrical engineering from TH Nürnberg Georg-Simon-Ohm, Nuremberg, Germany, in 2015, and the M.Sc. degree in information and communication technologies from Friedrich-Alexander-Universität Erlangen-Nürnberg (FAU), Erlangen, Germany, in 2017.

From 2014 to 2016, he was a Research Assistant in the field of fiberoptic photonics with Siemens AG, Munich, Germany. After graduation, he joined the Institute of Microwaves and Photonics (LHFT), FAU, in 2017. His research interests include radar signal processing and radar hardware.

Andreas Hofmann received the M.Sc. degree in electrical engineering from Friedrich-Alexander-Universität Erlangen-Nürnberg (FAU), Erlangen, Germany, in 2016, where he is currently pursuing the Ph.D. degree.

In 2016, he joined the Institute of Microwaves and Photonics, FAU. His current research interests include MIMO radar, retrodirective transponders, and switched injection-locked oscillators.

Christian Carlowitz (Member, IEEE) received the Dipl.-Ing. degree in information technology from the Clausthal University of Technology, Clausthal-Zellerfeld, Germany, in 2010, and the Dr.-Ing. degree from the Friedrich-Alexander-Universität Erlangen-Nürnberg (FAU), Erlangen, Germany, in May 2018, for his thesis on "wireless high-speed communication based on regenerative sampling."

He is currently with the Institute of Microwaves and Photonics, FAU, where he has led the "Microwave and Photonic Systems" Group since 2018. His research interests include the conception, design, and implementation of innovative system architectures for radar and communication frontends at microwave, mm-Wave, and optical frequencies. He focuses especially on hardware concepts, and analog and digital signal processing techniques, for ultra-wideband high-speed communication systems, full-duplex mobile communication transceivers, and massive MIMO base stations, and for ranging and communication with mm-Wave RFID systems.

Dr. Carlowitz is a member of the IEEE Microwave Theory and Techniques Society (MTT-S). He also serves as a member of the IEEE MTT-S Technical Committee "RF/Mixed-Signal Integrated Circuits and Signal Processing" (MTT-15). He is also a Regular Reviewer of the IEEE TRANSACTIONS ON MICROWAVE THEORY AND TECHNIQUES journal. He is also a member of the International Microwave Symposium (IMS) Technical Program Review Committee, and a regular reviewer for several additional international conferences, including EuMW and ICMIM.

Martin Vossiek (Fellow, IEEE) received the Ph.D. degree from Ruhr-Universität Bochum, Bochum, Germany, in 1996.

In 1996, he joined Siemens Corporate Technology, Munich, Germany, where he was the Head of the Microwave Systems Group from 2000 to 2003. Since 2003, he has been a Full Professor with Clausthal University, Clausthal-Zellerfeld, Germany. Since 2011, he has also been the Chair of the Institute of Microwaves and Photonics (LHFT), Friedrich-Alexander-Universität Erlangen-Nürnberg (FAU), Erlangen, Germany. He has authored or coauthored more than 300 articles. His research has led to over 90 granted patents. His current research interests include radar, transponder, RF identification, communication, and wireless locating systems.

Dr. Vossiek is currently a member of the German National Academy of Science and Engineering (acatech) and the German Research Foundation (DFG) Review Board. He is also a member of the German IEEE Microwave Theory and Techniques (MTT)/Antennas and Propagation (AP) Chapter Executive Board and the IEEE MTT Technical Committees MTT-24 Microwave/mm-Wave Radar, Sensing, and Array Systems; MTT-27 Connected and Autonomous Systems (as the Founding Chair); and the MTT-29 Microwave Aerospace Systems. He also serves on the Advisory Board of the IEEE CRFID Technical Committee on Motion Capture & Localization. He is also a member of organizing committee and technical program committee for many international conferences. He has served on the review boards for numerous technical journals. He received more than ten best paper prizes and several other awards. For example, he was awarded the 2019 Microwave Application Award from the IEEE MTT Society (MTT-S) for Pioneering Research in Wireless Local Positioning Systems. From 2013 to 2019, he was an Associate Editor of the IEEE TRANSACTIONS ON MICROWAVE THEORY AND TECHNIQUES (MTT).